optical amplifier (SOA). The phase conjugated signal is produced by four-wave mixing. The wavelength shift in the SOA-OPC is −10nm. The converted signal is filtered out in two stages of 3nm filter and amplified by an EDFA. The measured conversion efficiency is −20.5dB [4]. In this system, it is assumed that the condition $\beta_2^{(1)} z_1 = \beta_2^{(2)} z_2$ is satisfied, where the amounts of total dispersion in both sections are the same. The lengths of the transmission fibres in each section are z_1 = 51.0km and z_2 = 53.5km. The dispersion values are $\beta_2^{(1)}$ = −21.5ps²/km (at 1550.5nm) and $\beta_2^{(2)}$ = −20.5ps²/km (at 1540.5nm). The input powers P_{in} at the position indicated in Fig. 1*b* are set to be equal. The signal is detected with a 50GHz *pin* photodetector. The electrical signal is mixed down with the LO, demodulated, and directed to the BER tester.

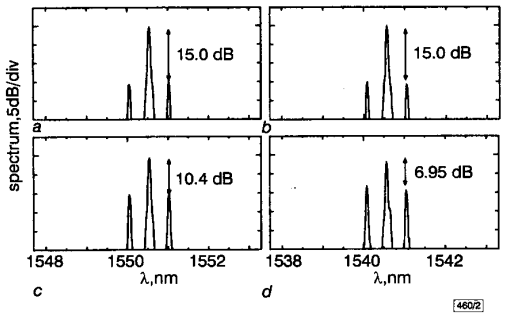

Fig. 2 *Measured optical spectra at midway OPC and at output, when input power P_{in} is 5dBm, and measured optical spectra at midway OPC and at output, when input power P_{in} is 15dBm*

a Midway OPC, P_{in} = 5dBm
b Output, P_{in} = 5dBm
c Midway OPC, P_{in} = 15dBM
d Output, P_{in} = 15dBm

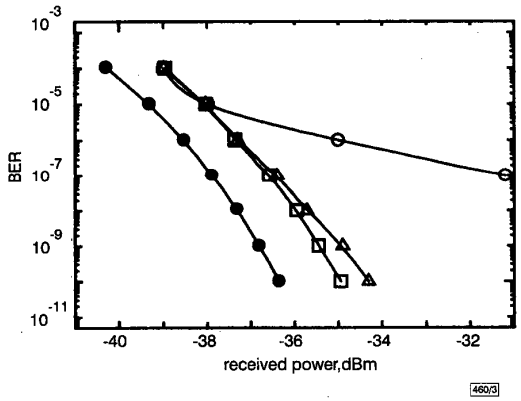

Fig. 3 *Measured BER against received optical power*

□ Pin = 5dBm
△ Pin = 10dBm
○ Pin = 15dBm
● back-to-back
z_1 = 51km (at 1550.5nm), z_2 = 53.5km (at 1540.5nm)

Fig. 2*a* and *b*, respectively, show the spectra at the midway OPC and at the output of the system when the input power P_{in} = 5dBm. The nonlinear length L_{NL}, as defined by $1/\gamma P_{av}$, is calculated to be 306km. In this case, the transmission lengths z_1 and z_2 are much shorter than L_{NL}. No change in the optical spectrum is observed at both positions. Fig. 2*c* shows the optical spectrum at the midway OPC when P_{in} = 15dBm. In this case, L_{NL} is 30.6km and the transmission lengths z_1 and z_2 are longer than L_{NL}. The modulation depth, which can be observed by the power ratio of the sideband to the carrier light, becomes higher after the propagation compared with the case of P_{in} = 5dBm. This is because of the modulational instability [5, 6], which is induced by the small modulation of the 60GHz millimetre-wave data signal. Four-wave mixing in the anomalous dispersion regime along with SPM causes modulational instability. In an ideal OPC system, the modulational instability that occurs in the first section can be compensated for in the second section. In a practical OPC system, however, the power change is not symmetric with respect to the OPC position, which results in distorted optical spectra. The degree of imperfect compensation becomes larger as the input power increases. Fig. 2*d* shows the output spectra when P_{in} is 15dBm. The distorted spectrum caused by the modulational instability is also observed despite the use of the midway OPC. Compared with the case in which the midway OPC is not inserted, where the power of the sideband is only −5.65dB below the carrier, the distortion caused by GVD and SPM is partially compensated for by the midway OPC. The measured BERs are plotted in Fig. 3. No error floor is observed when the input power is < 5.0dBm. With increasing input power, the error floor is clearly observed. The error floor is produced by the asymmetric power change. A comparison of L_{NL} with the transmission lengths z_1 and z_2 shows that the OPC must be inserted at the position where the transmission length is much less than the nonlinear length.

Conclusion: We have observed the limitation of the midway OPC system applied for 60GHz SCM optical DSB signal transmission. The BER degradation was caused by the asymmetry of the power change in the sections of fibre on either side of the OPC. These results indicate that the transmission length before and after the OPC must be much less than the nonlinear length.

2 March 1999
Electronics Letters Online No: 19990588
DOI: 10.1049/el:19990588

H. Sotobayashi and K. Kitayama (*Communications Research Laboratory, Ministry of Posts and Telecommunications, Lightwave Network Section, Photonic Technology Division, 4-2-1, Nukui-Kita, Koganei, Tokyo 184-8795, Japan*)

E-mail: soba@crl.go.jp

K. Kitayama: Now with Osaka University, Department of Electronics and Information Systems, Graduate School of Engineering, Osaka, Japan

References

1 WATANABE, S., NAITO, T., and CHIKAMA, T.: 'Compensation of chromatic dispersion in a single-mode fiber by optical phase conjugation', *IEEE Photonics Technol. Lett.*, 1993, **5**, pp. 92–95
2 MESLENER, G.J.: 'Chromatic dispersion induced distortion of modulated monochromatic light employing direct detection', *IEEE J. Quantum Electron.*, 1984, **QE-20**, pp. 1208–1216
3 MARTI, J., and RAMOS, F.: 'Compensation for dispersion-induced nonlinear distortion in subcarrier systems using optical-phase conjugation', *Electron. Lett.*, 1997, **33**, pp. 792–794
4 KITAYAMA, K., and SOTOBAYASHI, H.: 'Fading-free fiber-optic transport of 600Hz-optical DSB signal by using in-line phase conjugator'. Optical Fiber Communication Conf. (OFC '99), San Diego, February 1999, Paper WD4
5 HASEGAWA, A., and BRINKMAN, W.F.: 'Tunable coherent IR and FIR sources utilizing modulational instability', *IEEE J. Quantum Electron.*, 1980, **QE-16**, (7), pp. 694–697
6 HASEGAWA, A.: 'Generation of a train of soliton pulses by induced modulational instability in optical fibers', *Opt. Lett.*, 1984, **9**, (7), pp. 288–290

High-speed operation of travelling-wave electroabsorption modulator

V. Kaman, S.Z. Zhang, A.J. Keating and J.E. Bowers

The authors describe the high-speed operation of an electroabsorption modulator with travelling-wave electrodes. The modulator exhibited good performance over a broad bandwidth in 10 and 30Gbit/s transmission experiments. The polarisation-insensitive electroabsorption modulator required a low switching voltage of ~ $1.6V_{p-p}$.

Introduction: The speed of optical fibre telecommunication systems based on electrical time division multiplexing has increased rapidly over the last decade enabling 40Gbit/s throughput for a single carrier [1, 2]. Electroabsorption (EA) modulators with very low driving voltage, high modulation efficiency, polarisation insensitivity

and integrability with lasers [3 – 6], make them very attractive devices for optical communications systems. The bandwidth of EA modulators based on a lumped-electrode structure is limited by the total capacitance; short lengths result in high bandwidths while longer devices exhibit better extinction ratios, necessitating a tradeoff between bandwidth and extinction ratio. Recently, it has been shown that longer devices with potentially lower drive voltages and increased extinction ratio can be achieved using a travelling-wave electrode structure that overcomes the RC limitation [7, 8].

We have recently demonstrated a polarisation-insensitive travelling-wave EA modulator operating at 1.55μm, with a bandwidth of 25GHz and a 20dB extinction ratio (DC) voltage of 1.20 and 1.28V for the TE and TM modes, respectively [9]. In this Letter, we report on the 10 and 30Gbit/s operation of this modulator.

Modulator characteristics: The travelling-wave EA modulator used in this experiment is similar to the device described in [9]. The device was designed to be polarisation-insensitive over a range of wavelengths. The fibre-to-fibre insertion loss was 16dB at 1542nm. A drive voltage of 2V was required for a maximum extinction ratio (DC) of 30dB. The 25GHz bandwidth was achieved by terminating the travelling-wave electrode in a low resistance using a thin-film resistor.

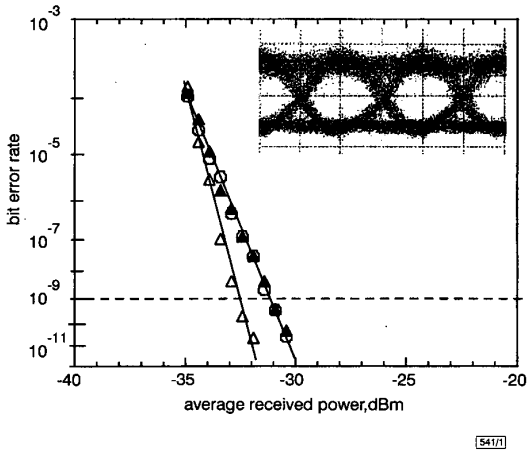

Fig. 1 *Bit error rate curves for 10Gbit/s transmission*

Inset: Received eye diagram after 150km transmission (H: 50ps/div, V: 80mV/div)
▲ back-to-back, TM mode
○ back-to-back, TE mode
△ 150km DSF transmission

10Gbit/s transmission: Transmission experiments using the travelling-wave EA modulator at 10Gbit/s were carried out (2^{31}–1 pattern length) with commercially available components. A drive voltage of ~ $1.6V_{p-p}$ was applied to the EA modulator by high-speed probes. A DFB laser operating at 1542nm followed by a polarisation controller was used as the light source into the EA modulator. Two lens pairs were used to couple the light into and out of the modulator. The output signal from the EA modulator was amplified by an erbium-doped fibre amplifier (EDFA) before it was launched into 150km of dispersion-shifted fibre (DSF) with a mean dispersion parameter of –0.93ps/(nm-km). The α parameter of the modulator was +1.2 at the operating bias of –1.1V. Fig. 1 shows the bit error rate (BER) performance of the EA modulator for back-to-back and > 150km of DSF. In the back-to-back measurements, error-free operation and a sensitivity of –31.2dBm were achieved for both the TM and the TE polarisations without changing the operating conditions of the modulator. This indicates that the polarisation dependence of the EA modulator is very low. An improved sensitivity of –32.8dBm was achieved after 150km DSF transmission due to the interplay between the positive chirp of the modulator and the slightly negative dispersion of the fibre. The inset in Fig. 1 shows the received eye diagram after transmission over 150km of DSF fibre. The long pattern length used in this transmission indicates the good low-frequency characteristics for this modulator.

30Gbit/s transmission: To explore the higher-speed characteristics of the EA modulator, transmission experiments at 30Gbit/s were carried out using the setup shown in Fig. 2. The 30Gbit/s NRZ electrical signal was generated by multiplexing four 7.5Gbit/s (2^7–1 pattern length) data streams delayed by 10 bits from each other using a 4:1 multiplexer (MUX) [10]. The pattern length was limited by the receiver electronics; however, excellent low frequency performance of the EA modulator was confirmed with the 10Gbit/s transmission experiment described earlier. At the receiver, an EDFA was used as an optical preamplifier into the packaged receiver with a 30GHz bandwidth [11]. Broadband electrical amplifiers followed the optical receiver and the signal was fed into a 30Gbit/s 1:4 demultiplexer (DMUX) and a clock recovery circuit (CRC) [10].

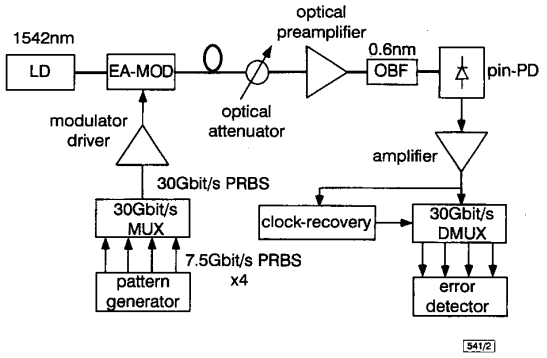

Fig. 2 *Schematic diagram of 30Gbit/s setup*

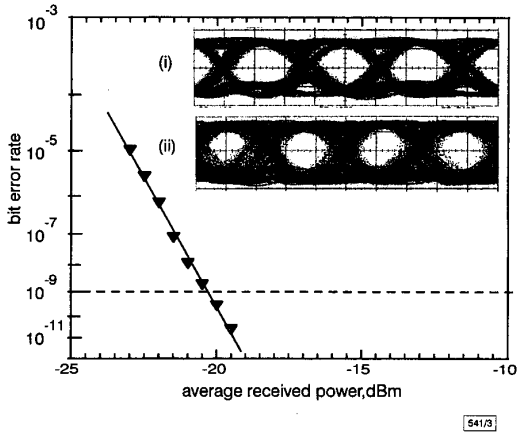

Fig. 3 *Bit error rate for back-to-back 30Gbit/s transmission*

Inset: (H: 13ps/div, V: 100mV/div)
(i) 30Gbit/s output signal from 4:1 MUX
(ii) received back-to-back 30Gbit/s signal

Fig. 3 shows the BER performance of the travelling-wave EA modulator for back-to-back transmission at 30Gbit/s. Error-free operation and an optical sensitivity of –20.2dBm were achieved for the best demultiplexed channel. The inset in Fig. 3 shows (*a*) the 30Gbit/s output of the 4:1 MUX and (*b*) the received 30Gbit/s signal after back-to-back transmission. The slight eye closure on every other channel, we believe, is due to an on-chip clock-phase alignment problem in the electrical MUX. Improvement in the 30Gbit/s optical sensitivity should be possible by improving the receiver and the fibre coupling into and out of the EA modulator.

Summary: We have successfully demonstrated 10 and 30Gbit/s operation of a travelling-wave EA modulator. These experiments confirmed a broad bandwidth and a low switching voltage for these modulators. Our results indicate that travelling-wave EA modulators, with their low driving voltage and polarisation-insensitivity, are strong candidates for future high-speed optical communication systems.

Acknowledgment: This work was supported by DARPA under the MOST and ULTRA programs.

12 April 1999
Electronics Letters Online No. 19990671
DOI: 10.1049/el:19990671

V. Kaman, S.Z. Zhang, A.J. Keating and J.E. Bowers (*Department of Electrical and Computer Engineering, University of California, Santa Barbara, CA 93106, USA*)

E-mail: kaman@opto.ucsb.edu

References

1 BOGNER, W., GOTTWALD, E., SCHOPFLIN, A., and WEISKE, C.-J.: '40 Gbit/s unrepeatered optical transmission over 148 km by electrical time division multiplexing and demultiplexing', *Electron. Lett.*, 1997, **33**, pp. 2136–2137

2 HAGIMOTO, K., YONEYAMA, M., SANO, A., HIRANO, A., KATAOKA, T., OTSUJI, T., SATO, K., and NOGUCHI, K.: 'Limitations and challenges of single-carrier full 40-Gbit/s repeater system based on optical equalization and new circuit design'. OFC '97 Tech. Dig., 1997, Paper ThC1, pp. 242–243

3 YOSHINO, K., WAKITA, K., KOTAKA, I., KONDO, S., NOGUCHI, Y., KUWANO, S., TAKACHIO, N., OTSUJI, T., IMAI, Y., and ENOKI, T.: '40 Gbit/s operation of InGaAs/InAlAs MQW electroabsorption modulator module with very low driving-voltage'. Proc. ECOC '96 Tech. Dig., 1996, pp. 203–206

4 TAKEUCHI, H., TSUZUKI, K., SATO, K., YAMAMOTO, M., ITAYA, Y., SANO, A., YONEYAMA, M., and OTSUJI, T.: 'NRZ operation at 40Gb/s of a compact module containing an MQW electroabsorption modulator integrated with a DFB laser', *IEEE Photonics Technol. Lett.*, 1997, **9**, pp. 572–574

5 IDO, T., TANAKA, S., and INOUE, H.: 'MQW electroabsorption modulators for 40-Gbit/s TDM systems'. OFC '97 Tech. Dig., 1997, Paper WG5, pp. 140–141

6 DEVAUX, F., BORDES, P., OUGAZZADEN, A., CARRE, M., and HUET, F.: 'Experimental optimisation of MQW electroabsorption modulators with up to 40GHz bandwidths', *Electron. Lett.*, 1994, **30**, pp. 1347–1348

7 KAWANO, K., KOHTOKU, M., UEKI, M., ITO, T., KONDOH, S., NOGUCHI, Y., and HASUMI, Y.: 'Polarisation-insensitive travelling-wave electrode electroabsorption (TW-EA) modulator with bandwidth over 50GHz and driving voltage less than 2V', *Electron. Lett.*, 1997, **33**, pp. 1580–1581

8 JAGER, D., STOHR, A., and HEINZELMANN, R.: 'Advanced microwave photonic devices for analog optical links'. 1998 Int. Topical Meeting on Microwave Photonics (MWP'98), 1998, Paper TuC1, pp. 153–156

9 ZHANG, S., CHIU, Y., ABRAHAM, P., and BOWERS, J.: '25GHz polarization-insensitive electroabsorption modulators with traveling-wave electrodes', *IEEE Photonics Technol. Lett.*, 1999, **11**, pp. 191–193

10 RUNGE, K., ZAMPARDI, P.J., PIERSON, R.L., THOMAS, P.B., BECCUE, S.M., YU, R., and WANG, K.C.: 'High speed AlGaAs/GaAs HBT circuits for up to 40Gb/s optical communication'. IEEE GaAs Symp., 1997, pp. 211–214

11 PETERSEN, A.K., REYNOLDS, T., NAGARAJAN, R., WEY, Y.-G., BOWERS, J.E., and RODWELL, M.: '3MHz – 30GHz traveling-wave optical front-end receiver'. OFC '95 Tech. Dig., 1995, Paper WM4, pp. 157–158

Increased input power dynamic range of Mach-Zehnder wavelength converter using a semiconductor optical amplifier power equaliser with 8dBm output saturation power

J.-Y. Emery, B. Lavigne, C. Porcheron, C. Janz, F. Dorgeuille, F. Pommereau, F. Gaborit, I. Guillemot-Neubauer and M. Renaud

A two-section semiconductor optical amplifier is proposed and investigated for use as a power equaliser, providing a 3dB output saturation power of 8 ± 1dBm. Using the device to control the input power of a Mach-Zehnder wavelength converter, an increase in the input power dynamic range of the converter from 2.5 to > 20dB is demonstrated at 10Gbit/s.

Introduction: Semiconductor optical amplifiers (SOAs) are promising devices for optical system applications such as amplification, switching and wavelength conversion. Recently, a power equalisation function has been identified as important in order to increase the low input power dynamic range of optical wavelength converters based on interferometric structures [1 – 3]. Single SOA devices can provide power equalisation, but the usable output power is limited because of the dependence of the output saturation power on the driving current. As a consequence, the input power dynamic range of the equaliser is also limited. By cascading two optical amplifiers the capability of increasing the output power saturation of the power equaliser has been demonstrated [2, 4]. In such a device, the input signal power is controlled by the first amplifier while the second amplifier maintains a sufficient gain and a high output saturation power. By cascading an SOA and an Er-doped fibre amplifier, the input power dynamic range of an interferometric wavelength converter has previously been increased from 3 to 28dB [1]. Recently, 5 dBm output saturation power has been demonstrated in a two-section SOA based on a multiquantum well structure [4].

In this Letter, we report an optical power equaliser based on a two-section SOA which provides 8dBm output saturation power. 10Gbit/s experiments with NRZ signal have been carried out using the two-section SOA to control the input power of a Mach-Zehnder interferometer (MZI) wavelength converter. Control of the bias current in the first section enables us to increase the input power dynamic range of the MZI from 2dB to > 20dB with a sensitivity penalty of < 1dB.

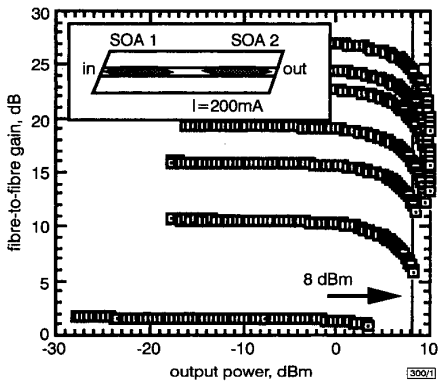

Fig. 1 *Fibre-to-fibre gain against output power measured at 1.55μm for different bias currents in first section of SOA power equaliser*

Inset: schematic diagram of two section SOA with passive waveguide in between
From top to bottom: Bias current = 200, 100, 80, 60, 50, 40, 30mA

Device principle and design: The power equaliser is based on a two-section SOA (inset Fig. 1). In such a device, the bias current of the first section allows us to control the optical power entering into the second section. In the second section, a high current is maintained in order to provide a sufficient gain and a high output power. To accept a high input signal power, the input SOA has to work in a near-transparent regime. In this regime the noise figure increases rapidly, leading to a reduction in the output optical signal-to-noise ratio. The noise figure can be limited by either decreasing the cavity length of the SOA or by decreasing the optical confinement factor of the active layer. The device shown in Fig. 1 is realised by a combination of these two approaches. The polarisation-insensitive SOA structure is based on a low-tensile strained bulk separate confinement heterostructure [5] with an active layer thickness of 0.12μm, giving an optical confinement factor of ~0.25. The active buried ridge stripe is 800μm in total length including 150μm long tapered sections at both ends. A double core taper consisting of the tapered active region and an underlying passive waveguide enables us to couple the two SOAs. The passive section, in between the two SOAs, provides electrical insulation of the electrodes and an attenuation function. This attenuation due to propagation losses (5–7dB) limits the gain saturation of the second amplifier by the amplified spontaneous emission emitted from the first SOA (and reciprocally). The overall device length is 2.4mm including passive waveguides at each end which provide typical full beam divergences of 13° × 15° [6].